A New Paradigm for Local and Sustained Release of Therapeutic Molecules to the Injured Spinal Cord for Neuroprotection and Tissue Repair

Catherine E. Kang, M.S.,[1,2] Peter C. Poon, B.Sc.,[1] Charles H. Tator, M.D., Ph.D.,[3] and Molly S. Shoichet, Ph.D.[1,2,4]

After spinal cord injury (SCI), a complex cascade of events leads to tissue degeneration and a penumbra of cell death. Neuroprotective molecules to limit tissue loss are promising; however, intravenous delivery is limited by the blood–spinal cord barrier and short systemic half-life. Current local delivery strategies are flawed: bolus injection results in drug dispersion throughout the intrathecal (IT) space, and catheters/pumps are invasive and open to infection. Our laboratory previously developed a hydrogel of hyaluronan (HA) and methylcellulose (MC) (HAMC) that, when injected into the IT space, was safe and, remarkably, had some therapeutic benefit on its own. In order to test this new paradigm of local and sustained delivery, relative to conventional delivery strategies, we tested, for the first time, the *in vivo* efficacy of HAMC as an IT drug delivery system by delivering a known neuroprotective molecule, erythropoietin (EPO). *In vitro* studies showed that EPO was released from HAMC within 16 h, with 80% bioactivity maintained. When the material alone was injected *in vivo*, individual fluorescent labels on HA and MC showed that HA dissolved from the gel within 24 h, whereas the hydrophobically associated MC persisted in the IT space for 4–7 days. Using a clip compression injury model of moderate severity, HAMC with EPO was injected in the IT space and, in order to better understand the potential of this delivery system, compared to the therapeutic effect of both common delivery strategies—IT EPO and intraperitoneal EPO—and a control of IT HAMC alone. IT HAMC delivery of EPO resulted in both reduced cavitation after SCI and a greater number of neurons relative to the other delivery strategies. These data suggest that the localized and sustained release of EPO at the tissue site by HAMC delivery enhances neuroprotection. This new system of IT delivery holds great promise for the safe, efficacious, and local delivery of therapeutic molecules directly to the spinal cord.

Introduction

TREATMENT FOR THE DEVASTATING condition of spinal cord injury (SCI) is currently limited, in part due to the complexity of the pathophysiology after trauma and the lack of effective therapies.[1] After an initial traumatic injury to the spinal cord, a cascade of events causes further tissue damage. This process is termed the secondary injury and is characterized by ischemia, hemorrhage, inflammation, and edema within the cord. These secondary events traumatize a large area of tissue that was previously unaffected or sublethally affected by the primary insult, and is thought to be responsible for the significant further loss of function that occurs after SCI.[2] Recent research has focused on administering neuroprotective agents to interrupt this cascade, thereby minimizing tissue degeneration.

High doses of therapeutic agents are required to cross the blood–spinal cord barrier (BSCB) and reach the site of injury when delivered by the traditional systemic route, often leading to widespread side effects. Often only a brief period of delivery is achieved due to renal clearance and the short half-life of molecules in blood. These limitations suggest that localized delivery of these agents would result in greater neuroprotection and tissue sparing. Bolus delivery of therapeutic agents to the intrathecal (IT) space has been investigated; however, the therapeutic window is short due to drug clearance by cerebrospinal fluid (CSF) flow and absorption.[3,4] Osmotic minipumps became popular in the last decade for localized and sustained experimental delivery of drugs to the IT space, and implanted pumps have been used in humans for the delivery of analgesics and other agents.[5] However, widespread utilization of pumps has been slow

[1]Department of Chemical Engineering and Applied Chemistry, University of Toronto, Toronto, Canada.
[2]Institute of Biomaterials and Biomedical Engineering, Toronto, Canada.
[3]Department of Surgery, Krembil Neuroscience Centre, Toronto Western Research Institute, University of Toronto, Toronto, Canada.
[4]Department of Chemistry, University of Toronto, Toronto, Canada.

due to catheter blockage, infections, and formation of proliferative lesions around the insertion site.[6] Our laboratory has pioneered an injectable, polymeric drug delivery system for IT drug administration whereby therapeutic agents dispersed throughout a fast-gelling polymer can be released directly at the site of injury.[7,8] A new material blend of 2% hyaluronan (HA) and 7% methylcellulose (MC) (HAMC) was developed and shown to be fast gelling within the IT space, minimally invasive by injection through a 30G needle, noncell adhesive, biodegradable, and biocompatible *in vivo*.[9] The goal herein was to test the potential of this new paradigm of IT HAMC delivery to conventional IT bolus and intraperitoneal (IP) delivery strategies.

Methylprednisolone, a steroid administered systemically, is one of the few agents that can cross the BSCB and shown to have a positive effect on recovery in clinical trials, although there was only a mild benefit[10] and the trials have been widely criticized.[11,12] Many other therapeutic agents are being investigated that show reduced apoptosis in several cell types,[13,14] reduced demyelination,[15,16] and reduced inflammation,[17,18] among others. These effects may directly prevent or indirectly lead to sparing of neurons, which can result in greater remodeling of the sensory and motor spinal tracts to improve functional recovery postinjury. Recent reports show that the hematopoietic protein erythropoietin (EPO) and EPO receptors, which play a role in central nervous system (CNS) development, are upregulated in the brain and spinal cord within minutes to hours after injury.[19,20] EPO has shown very positive functional recovery in stroke models, and the neuroprotective benefit of this glycoprotein has been proven in hypoxic and ischemic neonatal and adult rat brains.[21–24] Various groups have also shown a neuroprotective benefit of EPO in SCI, both in ischemic and compressive/contusive models.[13,20,25,26] The exact neuroprotective mechanism of EPO after SCI is still unclear, but it is postulated that mechanisms may include reduction of ischemic damage,[13] reduction of inflammation,[27,28] and sparing of white matter tracts in the spinal cord.[25,29] EPO may also have more direct actions on neurons, oligodendrocytes, and astrocytes, all of which express receptors for this molecule.[19,30–32] Since EPO can cross the BSCB,[33] it was an ideal molecule to test in terms of delivery strategy in the context of neuroprotection after SCI. Since HAMC forms a loose polymer network, fast drug release from this material was expected; however, Gorio *et al.*[25] demonstrated that a single IP injection of EPO provided similar neuroprotective effects after SCI to repeated IP injections for several days, further emphasizing EPO as a choice to test in IT HAMC delivery.

The objective of this study was to investigate the benefit of IT HAMC delivery relative to conventional delivery strategies of IT and IP. EPO was chosen as the molecule to test in this new delivery paradigm because of its demonstrated neuroprotective effects. We first studied the *in vitro* release of EPO from HAMC to provide some insight into the time course of release *in vivo*. The *in vivo* degradation of HAMC was also determined to ensure a sufficient time window for *in vivo* EPO delivery. Finally, the *in vivo* tissue benefit of EPO delivered in HAMC was compared to the conventional delivery strategies of IT EPO alone and IP EPO alone, using IT HAMC alone as a control for the delivery vehicle. We hypothesized that the localized and sustained release

achieved with IT delivery of EPO in HAMC would result in greater neuroprotection and tissue sparing than the controls.

Materials and Methods

Media and cells were purchased from American Type Culture Collection (ATCC, Rockville, MD), and reagents were sterile filtered before use. Unless otherwise indicated, all chemicals were purchased from Sigma-Aldrich Chemical (Mississauga, ON) and used as received.

Material preparation

Sodium hyaluronate was purchased from Novamatrix (1.5×10^6 Da; Drammen, Norway) and sterilized prior to use. To sterilize HA, a 0.1% HA solution in Millipore deionized water (dH$_2$O) was filtered through a 0.22 μm PES filter (Nalgene, Rochester, NY). The solution was then lyophilized under sterile conditions by covering 50 mL tubes with nylon 0.22 μm filters (Millipore, Billerica, MA), producing sterile HA powder. MC was sterilized by autoclaving for 20 min at 120°C. Artificial CSF (aCSF) was prepared in dH$_2$O with 148 mM NaCl, 3 mM KCl, 0.8 mM MgCl$_2$, 1.4 mM CaCl$_2$, 1.5 mM Na$_2$HPO$_4$, and 0.2 mM NaH$_2$PO$_4$.[8]

Sterile HAMC was produced by mixing polymer solutions in a laminar flow hood. The MC powder was added to half of the appropriate amount of sterile filtered aCSF at 90°C and vortexed until all polymer particles were wetted. The remaining amount of aCSF was added cold at 4°C, and the solution was shaken on an ice bath for 30 min. HA powder was then added to the MC solution, vortexed, and allowed to dissolve overnight at 4°C. This resulted in a 2% HA and 7% MC solution.

In vitro *release of EPO from HAMC*

The EPO/HAMC blend was similarly prepared to that of HAMC, with EPO dissolved in cold aCSF and added to MC that was dispersed in hot aCSF prior to the addition of HA. This order of addition was important to achieve a well-mixed suspension of EPO in HAMC. The solution was then loaded into a Hamilton syringe and 10 μL injected into the bottom of Eppendorf tubes containing 100 μL of aCSF, thereby approximating the large ratio of CSF to HAMC that is expected *in vivo* by injection into the IT space. These samples were incubated at 37°C on an orbital shaker, and aCSF was fully removed and replaced with fresh aCSF at $t = 0$, 10, 20, and 40 min, and 1, 2, 4, 8, 16, 32, 64, and 128 h. An ELISA assay (Quantikine IVD EPO Kit; R&D Systems, Minneapolis, MN) performed in triplicate was used to determine the concentration of EPO in the aCSF that was removed at each time point.

Bioactivity of released EPO

A cellular assay was used to determine the activity of the released EPO on the basis of TF-1 cell proliferation in response to EPO. Cells were maintained in RPMI-1640 media with 10% fetal bovine serum, 1% penicillin/streptomycin, and 2 ng/mL of granulocyte macrophage–colony-stimulating factor (GM-CSF). A 10 μL aliquot of HAMC containing EPO was injected into 90 μL of culture media lacking GM-CSF. These samples were incubated for $t = 10$, 20, and 40 min, and 1, 2, 4, 8, and 16 h, and the media was fully transferred to a fresh plate. A TF-1 cell suspension was added to each sample to achieve a final cell density of 1×10^4 cells/mL in each well. A standard

curve was obtained using samples of EPO dissolved in media at known concentrations, and kept in similar conditions to those with EPO in HAMC. All cells were incubated for 2 days at 37°C and 5% CO_2, and cell density was then assayed with Cell Titer 96, a substrate metabolized into a colored product only by live cells. The absorbance was measured at 490 nm with a VERSAmax tunable microplate reader, and cell density was calculated. Based on the standard curve correlating expected cell density to known concentrations of EPO, the concentration of bioactive EPO released from HAMC was determined for samples collected at each time point.

Degradation of HAMC in vitro and in vivo

Using carbodiimide chemistry, HA was conjugated to a BODIPY-Fluorescein (BODIPY-FL) hydrazide and MC was conjugated to Texas Red hydrazide for visualization within the IT space. For HA conjugation, a 1% HA in dH_2O solution was adjusted to pH 4.6 and 1-ethyl-3-(3-dimethylaminopropyl) carbodiimide hydrochloride (EDC) was added at a 2:1 molar ratio to HA. N-hydroxysuccinimide (NHS) was added in a 1:1 molar ratio to EDC to stabilize the intermediate, and BODIPY-FL hydrazide was then added in a 1:4 molar ratio to HA.[34] This was allowed to react at room temperature for 24 h, and was then dialyzed overnight (12,000 MWCO; Spectrum laboratories, Los Angeles, CA) and sterilized as described above for unmodified HA. For MC, the hydroxyl groups were first modified to carboxyl groups with bromoacetic acid using a protocol obtained from Hermanson.[35] MC was added to 1 M bromoacetic acid in 3 M NaOH and reacted at room temperature for 1.5 h. The reaction was stopped by adding solid monobasic sodium phosphate and neutralizing with 6 N HCl, and fluorescent modification of MC was then performed as described above for HA, with Texas Red hydrazide used in place of BODIPY-FL hydrazide. MC was then dialyzed overnight and sterilized in the same way as unmodified MC. In the fluorescent HAMC solution, fluorescent HA accounted for 0.5% of the total HA in the blend, and fluorescent MC accounted for 1% of total MC in the blend, which was prepared by the same procedure as their unmodified counterparts.

To determine if degradation of the labeled material matched that of the unlabeled HAMC, the mass loss of each was determined over time in vitro. To maintain the ratio of HAMC to CSF expected in vivo, 100 μL of unlabeled HAMC or fluorescent HAMC was injected into 1 mL of aCSF, which was equilibrated to 37°C. At $t = 0$, 1, 2, 4, and 8 h, and 1, 2, 4, 7, and 14 days, aCSF was fully removed from the samples and the remaining material was lyophilized and weighed. Mass at each time was compared to that at $t = 0$ to determine material loss over time.

Animal procedures were performed in accordance with the Guide to the Care and Use of Experimental Animals developed by the Canadian Council on Animal Care and approved by the Animal Care Committee at the Research Institute of the University Health Network. Fifteen Sprague-Dawley rats (200–250 g; Charles River, Montreal, Canada) were anesthetized by inhalation of halothane, and a laminectomy was performed at the T1-2 vertebral level. Fluorescently labeled HAMC was injected intrathecally as described in Jimenez Hamann et al.[7] Following injection, the overlying muscles and fascia were sutured closed, and the rats were ventilated with pure oxygen and placed under a heat lamp for recovery. Buprenorphine was administered every 12 h for 3 days postsurgery for pain management.

At $t = 0$ (immediately after injection), 1, 2, 4, and 7 days, animals were administered a lethal dose of sodium pentobarbital, and a 2 cm section of the spinal cord was removed at the T1-2 level. Tissue was removed fresh to prevent the gel from dislodging during the fixation process. Cords were sectioned parasagittally and imaged on a Leica DMRB inverted microscope with Stereo Investigator Software, version 6. For each component of HAMC, the fluorescent area within a given intensity range was calculated for each image. Fluorescence loss observed over time was indicative of bulk hydrogel degradation, which was calculated according to Equation (1), where A_0 is the initial fluorescent area (at $t = 0$) within intensity limits and A_t is the fluorescent area at time t within the same intensity limits:

$$100\% - \left(\frac{A_0 - A_t}{A_0} \times \text{Scaling factor} \times 100\% \right) \tag{1}$$
$$= \% \text{ Flourescence remaining}$$

The loss of fluorescence was scaled according to the % of HA or MC that was labeled. For HA a scaling factor of 4 was used because 1/4 of the total HA was fluorescent-HA; for MC a scaling factor of 7 was used because 1/7 of the total MC was fluorescent-MC.

EPO efficacy study

The operative procedure for 47 Sprague-Dawley rats (220–300 g; Charles River) was performed as described in the degradation study, except that rats sustained an SCI before injection. SCI was performed with the aid of an operating microscope by placing a modified aneurysm clip calibrated to a closing force of 35 g on the spinal cord. The cord was acutely compressed with this clip for 60 s, as previously described.[36] Immediately following the injury, one of four injections (10 μL) was performed: (1) injection of HAMC containing EPO into the IT space ($n = 10$); (2) HAMC without EPO injection into the IT space ($n = 13$); (3) bolus injection of EPO into the IT space ($n = 12$); and (4) bolus injection of EPO into the IP cavity ($n = 12$). An injection volume of 10 μL was constant amongst all groups, and all EPO solutions were prepared at 100 IU/μL. Animal weights varied from 250 to 300 g, resulting in a dosage of 3500 ± 200 IU/kg. This dosage was used based on previous studies with EPO in SCI where an IP dosage of 5000 IU/kg produced the greatest functional benefit.[25] Previous work in our lab showed that IT injection of aCSF was comparable to HAMC injection, and therefore the aCSF group was excluded from this study.[9] Postsurgical care of rats was identical to that in the degradation study except that rat bladders were manually expressed three times daily.

Functional assessment. To determine the efficacy of EPO in enhancing motor behavior after injury, open field motor function was assessed using the Basso, Beattie, and Bresnahan (BBB) scoring method[37] daily for 1 week and then weekly thereafter for 6 weeks. Each hindlimb was ranked by two blinded observers and concurrently videotaped. BBB scores range from 0 (no hindlimb movement) to 21 (normal gait behavior) and are used to assess functional improvement after injury and treatment.

Histology and immunohistochemistry. Animals for the degradation study were sacrificed at $t = 0$ (immediately following injury), 1, 2, 3, and 5 days following IP injection of an overdose of sodium pentobarbital. Fresh tissue was harvested to prevent dislodging HAMC from the IT space, then cryoprocessed and stored at $-80°C$ until cut into $20\,\mu m$ parasagittal sections. Images were obtained at $10\times$ with a Leica DMRB inverted microscope and Stereo Investigator Software (version 6). The area of HA and MC at each time point was determined by pixel intensity using Image J software.

Animals for the EPO efficacy study were sacrificed 42 days after surgery and perfused intracardially with 4% paraformaldehyde under deep anesthesia. A 2 cm segment of spinal cord encompassing the injury site was harvested from each animal and cryoprocessed. Cords from three to four animals from each group were sectioned parasagittally at $20\,\mu m$ thickness, and every sixth section was stained with either (1) Luxol fast blue/hematoxylin and eosin (LFB/H&E) for general morphology and to assess cavity area (volume and area measurements were equivalent for the 35 g clip injury model that we have utilized here[38]), (2) ED-1 (activated macrophage stain), or (3) glial fibrillary acidic protein (GFAP–activated astrocyte stain). Images were taken at $5\times$ (LFB/H&E) or $10\times$ (ED-1, GFAP) with a Leica DMRB inverted microscope using Stereo Investigator Software (version 6), and sections in the maximal cavity area were analyzed for area of macrophages and astrocytic scar formation based on pixel intensity using Image J software. Cords from three other animals in each group were cross-sectioned at $20\,\mu m$ for 1 cm caudal to the injury, and every fourth section stained with NeuN (Neural cell body stain) or CC-1 (Oligodendrocyte stain) to assess sparing of these cell types caudal to the injury. Images were obtained at $20\times$ with an Olympus BX61 Microscope with Image Pro Plus Software (version 5.1). Neurons were counted manually, and oligodendrocytes were counted in Image Pro Plus, which counted only objects within limits on intensity and object size.

Statistical analysis

All statistics were performed using Microsoft Excel. One-way ANOVA followed by the Tukey's *post hoc* *t*-test was used to compare BBB scores of all groups. The Student's *t*-test was used to compare the maximal cavity area and neuron counts. Differences were accepted to be statistically significant at $p < 0.05$. All errors are given as standard deviations.

Results

In vitro *release of EPO from HAMC*

Prior to studying the therapeutic and tissue benefit of IT HAMC delivery of EPO relative to conventional delivery techniques, we investigated the *in vitro* release profile where the volume ratio of EPO/HAMC injected into aCSF mimicked that of the animal model. The release profile of EPO was investigated over 128 h using an ELISA assay, from which it was determined that 99% of EPO was released from HAMC during the first 16 h (Fig. 1A). Peppas and coworker[39] have previously established models showing that the amount of drug release is proportional to t^n, where n is indicative of the transport mechanism from polymeric drug delivery systems. In unidimensional diffusion-mediated re-

lease from a slab geometry, $n = 0.5$ and a linear relationship exists between drug release and $t^{0.5}$ for ~ 60–80% of release.[39] This is a good approximation for the HAMC hydrogel geometry both *in vitro* in a test tube where the gel is a flat slab and *in vivo* in the IT space where the polymer blend is bound by the spinal cord and the dura. In Figure 1B, cumulative release *in vitro* is plotted versus $t^{0.5}$ and a linear relationship is maintained for the first ~ 75% of release ($R^2 = 0.992$), providing evidence that EPO release from HAMC is diffusion mediated. Deviation from the model was
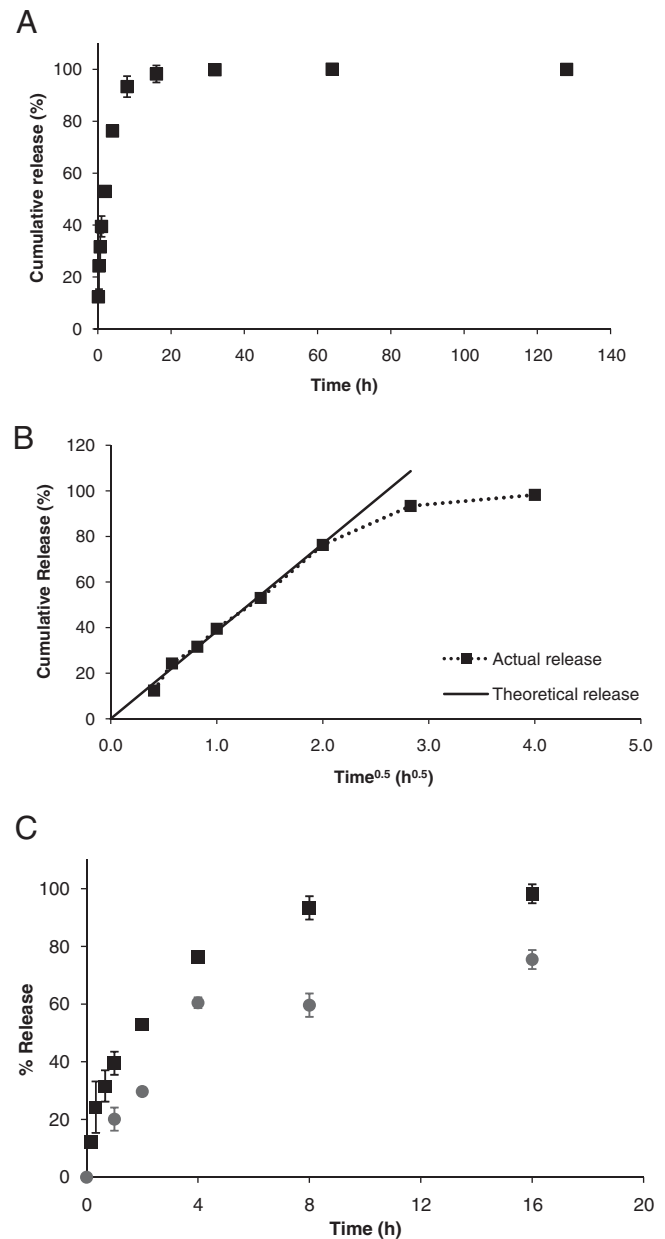
FIG. 1. (**A**) EPO release from HAMC over 128 h shows fast release within 16 h. (**B**) Cumulative release of EPO versus the square root of time demonstrates a diffusion-mediated release profile for the first 75% of EPO released. (**C**) EPO released from HAMC is 80% bioactive over time relative to cumulative EPO released. (■ = cumulative EPO released; ● = bioactive portion of EPO released).

expected for >80% release due to depletion of drug within the hydrogel, resulting in $n > 1$.[40]

A TF-1 cellular assay demonstrated that 80% of the released EPO remained bioactive over the 16 h release time (Fig. 1C). The ratio of bioactive EPO released to cumulative EPO released over time remained constant, showing that EPO bioactivity did not decrease with time. The 20% loss of activity was likely a result of the increased temperature needed to dissolve MC and obtain a good dispersion of EPO within HAMC. With most of the EPO released being bioactive, the therapeutic benefit of local IT delivery was investigated.

Degradation of HAMC *in vitro* and *in vivo*

Having established *in vitro* EPO release and bioactivity profiles from HAMC, we were interested in understanding the HAMC degradation profile *in vivo*. An *in vitro* degradation profile, shown in Figure 2A, demonstrated that fluorescently labeled HAMC had similar mass loss over time as that of the unlabeled material. Figure 2B shows longitudinal spinal cord sections where each of the HA and MC are labeled with a different fluorescent molecule. The profile of HAMC loss was followed over time by monitoring the change in area of fluorescence within the IT space. HA degraded quickly, exhibiting a ~95% loss in fluorescent area after 24 h. In contrast, MC showed an initial degradation of ~65% after 24 h and then continued to persist within the IT space for at least 4 days. After 7 days, traces of neither HA nor MC could be detected (Fig. 2C).

In vivo delivery of EPO with HAMC

To determine the efficacy of IT HAMC delivery relative to conventional IT bolus and IP delivery, EPO was chosen as the therapeutic molecule due to its known neuroprotective effects and ability to cross the BSCB, and then further compared to a control of IT HAMC alone. After SCI, secondary events that lead to inflammation and extensive cell death result in fluid accumulation or edema within the spinal cord.[41] Subsequently, a cyst or a cavity forms within the cord, filled with cellular debris and toxic factors.[42] The ultimate size of this fluid-filled cavity is proportional to the severity of the injury that is sustained, but the size may be reduced due to tissue sparing. To quantify any change in the size of the cavity due to HAMC or EPO, the maximal cavity area was measured in parasagittal histological sections stained with LFB/H&E (Fig. 3A). A reduction in the cavity area suggests tissue sparing, which is important for both neuroprotective and regenerative strategies. Figure 3B shows that the maximal cavity area for EPO delivered intrathecally from HAMC was significantly lower than that of the HAMC control ($p < 0.05$), demonstrating the benefit of IT HAMC delivery of EPO over HAMC alone. While not significantly different, IT HAMC delivery of EPO had less tissue loss than either IT EPO or IP EPO delivery. Thus, of the three delivery strategies, IT HAMC delivery of EPO resulted in the greatest tissue sparing, demonstrating the benefit of local and sustained release.

The general morphology of the tissue suggested that some cells may have been spared due to local delivery of EPO to the spinal cord. To determine which cells were spared, both neurons and oligodendrocytes were counted. Significantly higher numbers of neurons were counted in animals that
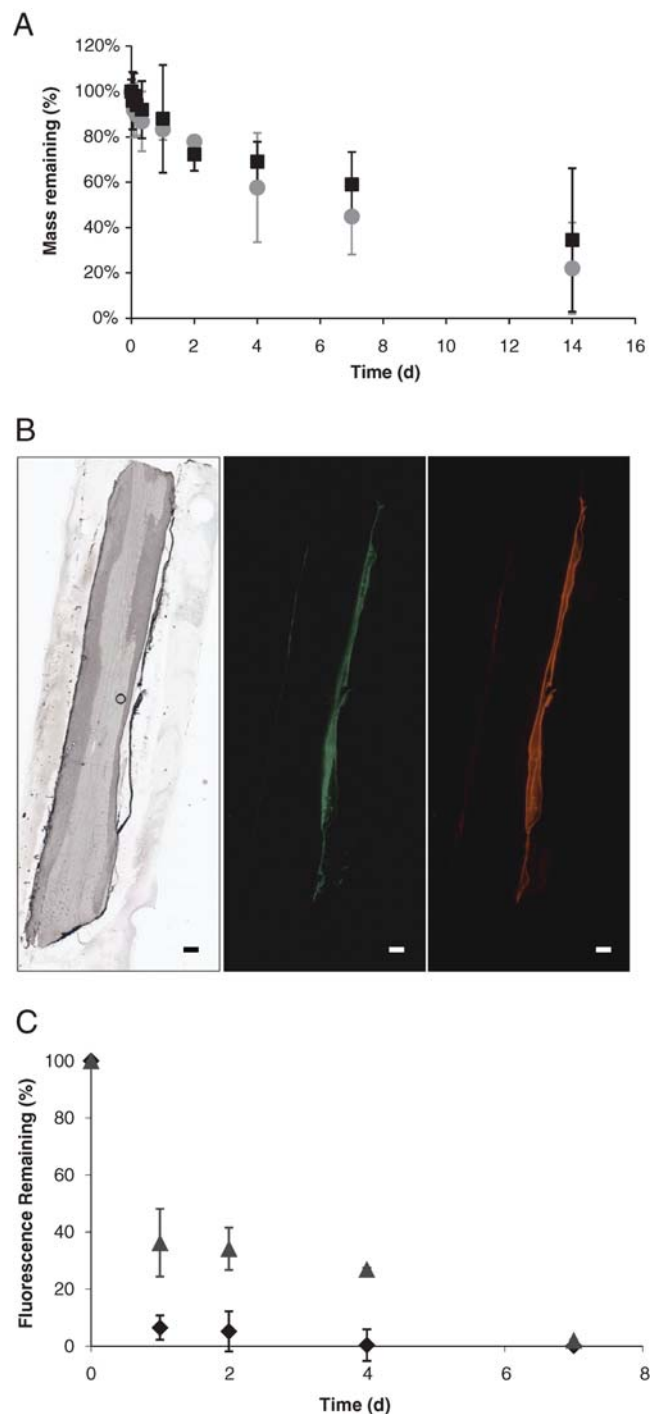

FIG. 2. (A) *In vitro* mass degradation is the same for labeled and unlabeled HAMC. (B) Brightfield image of a parasagittal spinal cord section (left) with corresponding fluorescent images of HA (middle) and MC (right) in the IT space immediately after injection. (C) EPO released from HAMC is 80% bioactive over time relative to cumulative EPO released. (■ = cumulative EPO released; ● = bioactive portion of EPO released). Color images available online at www.liebertonline.com/ten.
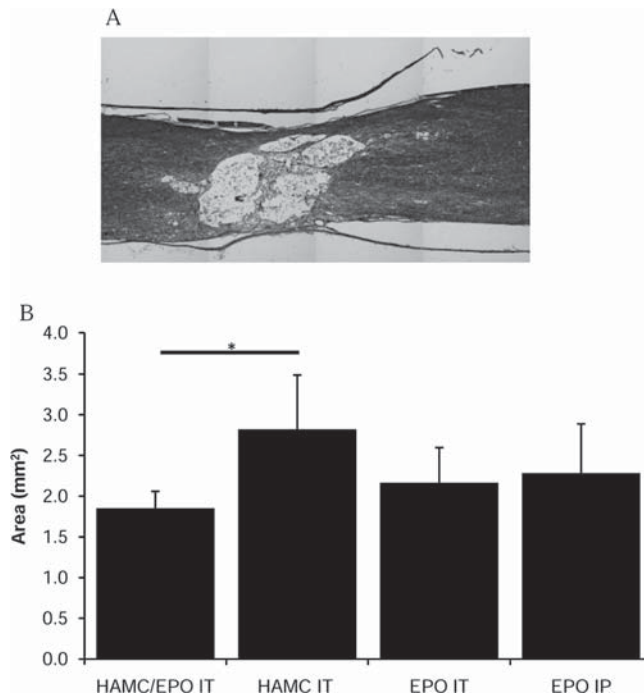
FIG. 3. (**A**) Parasagittal section of a representative spinal cord of an animal that received IT administration of EPO-loaded HAMC at maximal cavitation stained with LFB/H&E. (**B**) Comparison of maximal cavity area measured from parasagittal spinal cord sections ($n = 4$, mean + standard deviation; horizontal bars show statistical significant based on a t-test, $*p < 0.05$).

received IT HAMC delivery of EPO than animals that received EPO by either conventional route of delivery—IT bolus or IP (Fig. 4)—thereby showing an added tissue benefit of localized and sustained delivery with HAMC. Interestingly, bolus IT injection shows similar neuron counts to IP injection, substantiating studies that show EPO can cross the BSCB, particularly after an injury to the CNS.[33] IT HAMC alone resulted in highly variable neuron counts, demonstrating that its previously reported benefit[9] alone is insufficient to achieve neuroprotection.
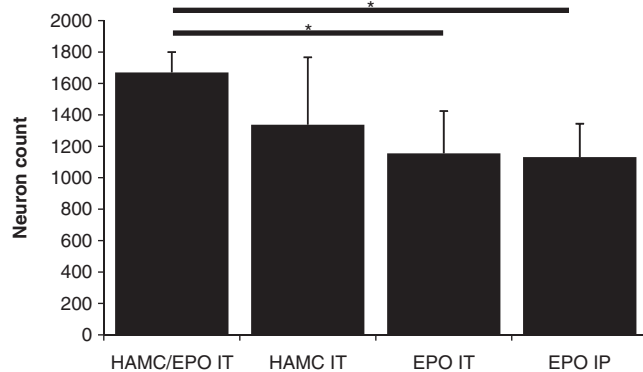
FIG. 4. Neuron counts observed in the ventral horns caudal to the injury site based on NeuN staining ($n = 3$, mean + standard deviation; horizontal bars show statistical significance based on t-test, $*p < 0.05$).
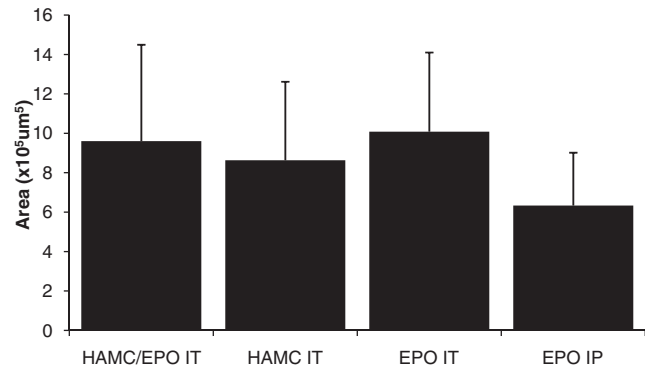

FIG. 5. Comparison of maximal inflammation area measured with ED-1 immunostaining of macrophages and microglia from parasagittal spinal cord sections ($n = 3$, mean + standard deviation).

Based on previous reports that describe white matter sparing with EPO delivery,[25] we postulated that there may also be a reduction in demyelination within the spinal cord, translating into a greater number of oligodendrocytes. However, oligodendrocyte counts showed no significant differences between any groups (data not shown). While it is generally known that reactive glial cells secrete factors that can lead to cell death, this action is more commonly associated with astrocytes than oligodendrocytes. Since no significant increase in oligodendrocytes or decrease in glial scar formation from reactive astrocytes (GFAP immunoreactivity, data not shown) was observed, it is unlikely that either of these indirect mechanisms of neuroprotection occurred. Combined with the neural sparing observed, these results suggest a more direct action of EPO binding to EPO receptors on neurons.

EPO has also been shown to decrease inflammation,[28] and for this reason ED-1 immunoreactivity was investigated (Fig. 5). ED-1 stains activated macrophages and microglia within the spinal cord, and the area over which these cells reside can be measured by pixel intensity of the images obtained. At the maximal cavity area, the total area of inflammation was measured, but EPO delivery did not appear to reduce the inflammatory area. Since it is possible for EPO delivered intraperitoneally to cross the BSCB, this small amount could decrease the macrophage response similar to EPO delivered intrathecally. Also, because inflammation was measured 6 weeks postinjury, the difference in the inflammatory response may have abated by this stage of recovery. Previous work with HAMC alone showed a significant decrease in inflammation relative to injection of aCSF without any therapeutic agents,[9] which was attributed to the wound healing property of HA.[43]

The functional benefit of EPO delivered with HAMC was tested by locomotor functional analysis using BBB scoring. Interestingly, at 7 days after EPO injection, animals that received IT HAMC delivery of EPO behaved significantly better than those that received IT bolus EPO ($p < 0.05$); however, in subsequent weeks, these animals behaved similarly to all other animals. Although Gorio et al.[25] showed a functional benefit with IP EPO injections, this study was later found to be irreproducible[44]; the present study also showed no functional benefit from EPO delivery, either IT or IP
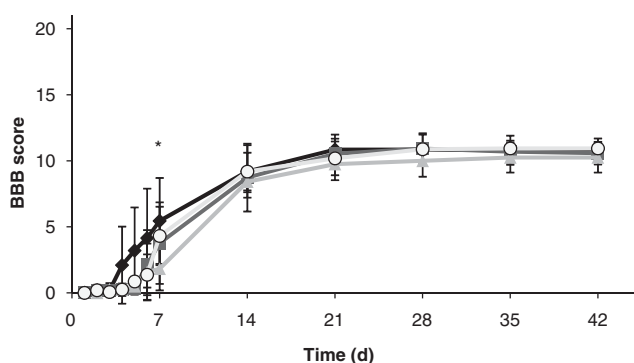
FIG. 6. Open field motor scores as assessed by the BBB scale over 6 weeks. Asterisk (*) shows statistical significance measured by ANOVA ($n = 9$–11, data shown as mean ± standard deviation). ◆ = IT administration of EPO-loaded HAMC; ■ = IT administration of HAMC alone; ▲ = IT administration of EPO; ○ = IP administration of EPO.

except at 7 days from HAMC (Fig. 6). The BBB scores were very similar for all groups, including those that received the control injection of HAMC alone. Within 3 weeks of injury, most animals had reached a plateau in functional recovery, with all animals exhibiting weight support of hindquarters.

Discussion

The diffusional release observed *in vitro* can be interpreted using a scaling argument where drug release for a characteristic time (τ) follows Equation (2):

$$\tau \sim \frac{L^2}{D_{drug}} \qquad (2)$$

where L is the characteristic length and D_{drug} is the diffusion coefficient of the drug.[45] The thickness of the gel was estimated at 2 mm based on the volume of gel and dimensions of the reservoir. The diffusion coefficient of the 30 kDa EPO molecule was estimated to be on the order of 1×10^{-10} m^2/s.[46] Thus, the characteristic diffusion time for EPO from HAMC is on the order of 10 h, consistent with the 16 h release observed experimentally. While this time scale is relatively short in the scheme of tissue remodeling that can occur for weeks or months after SCI, IT HAMC delivery of EPO likely has longer lasting effects on the tissue because the apparent concentration of EPO at the site of injury remains more than 100 times longer after injury when delivered with HAMC than either IT bolus or IP delivery of EPO, based on the average velocity of CSF flow.[47]

Upon injection *in vivo*, the temperature of HAMC increases from room temperature to 37°C, resulting in the formation of hydrophobic junctions of MC. These junctions act as physical crosslinks within the hydrogel, preventing fast dissolution of MC. However, an initial loss of MC is observed, with a slower degradation observed over a period of days. The initial 65% loss of MC in the first 24 h after injection may occur due to either quick dissolution prior to full gelation of MC or polydispersity of the MC chains, where lower molecular weight chains erode more quickly than higher molecular weight chains. Further, nonhomogeneous distribution of methyl groups on MC could result in

chains with only a few hydrophobic domains dissolving away more quickly, leaving only chains stabilized by several hydrophobic junctions.

The degradation of HAMC observed *in vivo* was faster than that observed *in vitro*, where degradation occurred over a period of 10–15 days. The difference may be due to continual CSF flow in the IT space, which amplifies the hydrogel dissolution rate. Also, the spatial constraints on the gel *in vivo* are greater than those *in vitro*; the spinal cord and dura limit gel layer thickness *in vivo*, and thinner slabs degrade more quickly due to increased disentanglement of polymer chains.[40] Importantly, the degradation of the fluorescently labeled HAMC was not statistically different from that of the unlabeled HAMC (Fig. 2A), validating the *in vivo* degradation results.

The rapid loss of HA from the hydrogel blend can be explained either by dissolution or degradation. Since HA forms crosslinks with neither MC nor itself, it is expected to dissolve away from the gel, assisted by CSF flow in the IT space. The natural enzyme hyaluronidase has a high specific activity for cleaving the N-acetyl-D-glucosamine in HA, and at concentrations found in serum,[48] it would degrade all of HA in HAMC within minutes of injection. Because this rate would cause complete loss of HA before tissue harvesting at initial time points and HA is present in the CSF,[49] it is unlikely that enzymatic degradation contributed significantly to the loss of HA in the IT space. This suggests that dissolution is likely the dominant mechanism for HA loss after injection into the IT space.

The concentration of EPO at the injury site is likely lowest for EPO delivered intraperitoneally due to dilution in the blood, presence of the BSCB, and CSF flow. Moreover, EPO causes red blood cell production,[50] and thus systemic administration can lead to thickening of the blood and increase the time needed to clear the hemorrhage after injury. These may account for the lack of neuroprotection after IP relative to IT HAMC delivery of EPO. Similarly, IT bolus delivery of EPO resulted in lower neuroprotection relative to IT HAMC delivery of EPO, likely due to the fast clearance by CSF flow. The improvement in neuron counts may be attributed to longer residence time and bioavailability of EPO released from HAMC at the site of injury combined with the wound-healing properties of HA. Spatial limitations of the hydrogel–spinal cord interface also cause a constant supply of EPO on the surface of the spinal cord, and EPO diffusing from HAMC into the cord in this manner may provide enhanced neuronal protection due to drug–receptor binding on the surface of neurons where EPO receptors are present.[31,51] Cultured primary neurons treated with EPO have been protected from excitotoxic cell death,[51] and experiments with EPO in stroke and traumatic brain injury models[24] have also shown this neuroprotective effect in hypoxic and ischemic environments.[23] While EPO delivery in HAMC showed greater neuroprotection than HAMC alone, the difference was not statistically significant; the high standard deviation in the HAMC group suggests that HAMC may play some role in neuroprotection, but not strong enough to reproducibly achieve neuron sparing. Together these data suggest a synergistic effect between the drug delivery system and the delivered molecule. We have shown here that EPO delivered locally with HAMC can increase neuronal sparing as compared to the traditional routes of drug delivery. The enhanced

tissue and neuron sparing achieved demonstrate the importance of our localized release strategy to limit degeneration and ultimately as a means to enhance functional recovery.

Behavioral recovery was significantly greater at 1 week postinjury for animals that received IT HAMC delivery of EPO relative to animals that received IT delivery of EPO alone; however, animals that received the bolus IT delivery of EPO alone had acute respiratory complications during surgery. Within 15–30 s of injection, animals that received an IT bolus injection of EPO alone began gasping deeply for breath, and after three to five gasps became apnoeic. Of the 16 rats undergoing surgery in this group, 12 exhibited this behavior, 4 of which could not be resuscitated, and died. The resuscitative efforts consisted of terminating anesthesia and applying external compression of the thoracic region until a pulse was identified and respiration restored. A recent report shows that slowed breathing is observed when EPO is administered in the CNS[52]; however, cessation of breathing was not listed as a side effect. This unexpected respiratory complication may have contributed to the lack of early functional recovery in this group. This was not observed in animals that received IP EPO or IT HAMC alone, but was observed for IT HAMC delivery of EPO in 2 of the 10 animals, both of which were successfully resuscitated. Interestingly, when the dose of the IT bolus EPO was reduced to 80%, to adjust for the bioactivity of EPO in HAMC, gasping was observed, but animals did not cease to breathe, suggesting that this effect is dose dependent. Although the enhanced locomotor functional benefit of EPO delivered via HAMC was only apparent at 7 days postinjury, delivery with HAMC allowed slower release of EPO and fewer respiratory complications relative to IT infusion of EPO alone. The functional benefit observed at 7 days may have occurred due to other secondary injury events such as reduced inflammation or decreased apoptosis at early time points; EPO has been shown to reduce the inflammatory response following traumatic brain injury[28,53,54] and decrease apoptosis.[28,54] The early improvement suggests that a localized delivery strategy with a longer release profile would sustain recovery further. This illustrates an added benefit of HAMC in terms of improved safety for IT drug administration and the potential for even greater functional recovery with prolonged delivery times.

In conclusion, the rate of dissolution of HAMC *in vivo* and the release rate of EPO *in vitro* suggests that this is a useful strategy for the localized release of neuroprotective molecules with an early therapeutic window. This work showed that IT HAMC delivery of EPO provided the greatest neuroprotective benefit in terms of tissue sparing after SCI. This was exemplified by decreased cavitation over HAMC alone and a greater number of spared neurons as compared to the IT EPO and IP EPO. Additionally, respiratory complications associated with EPO administration were minimized when delivered with HAMC. In ongoing studies, the IT HAMC delivery system is being further refined for prolonged degradation and release of other therapeutically relevant molecules with a focus on improving neuroprotection and regeneration after SCI.

Acknowledgments

References

1. Tator, C.H. Review of treatment trials in human spinal cord injury: issues, difficulties, and recommendations. Neurosurgery **59**(5), 957–982, 2006; discussion 982—987.
2. Hall, E.D., and Springer, J.E. Neuroprotection and acute spinal cord injury: a reappraisal. NeuroRx **1**(1), 80–100, 2004.
3. Terada, H., Kazui, T., Takinami, M., Yamashita, K., Washiyama, N., and Muhammad, B.A. Reduction of ischemic spinal cord injury by dextrorphan: comparison of several methods of administration. J Thorac Cardiovasc Surg **122**(5), 979–985, 2001.
4. Yaksh, T.L., Horais, K.A., Tozier, N., Rathbun, M., Richter, P., Rossi, S., Grafe, M., Tong, C., Meschter, C., Cline, J.M., and Eisenach, J. Intrathecal ketorolac in dogs and rats. Toxicol Sci **80**(2), 322—334, 2004.
5. Reynolds, L., Rauck, R., Webster, L., DuPen, S., Heinze, E., Portenoy, R., Katz, N., Charapata, S., Wallace, M., and Fisher, D.M. Relative analgesic potency of fentanyl and sufentanil during intermediate-term infusions in patients after long-term opioid treatment for chronic pain. Pain **110**(1–2), 182–188, 2004.
6. Jones, L.L., and Tuszynski, M.H. Chronic intrathecal infusions after spinal cord injury cause scarring and compression. Microsc Res Tech **54**(5), 317–324, 2001.
7. Jimenez Hamann, M.C., Tator, C.H., and Shoichet, M.S. Injectable intrathecal delivery system for localized administration of EGF and FGF-2 to the injured rat spinal cord. Exp Neurol **194**(1), 106–119, 2005.
8. Jimenez Hamann, M.C., Tsai, E.C., Tator, C.H., and Shoichet, M.S. Novel intrathecal delivery system for treatment of spinal cord injury. Exp Neurol **182**(2), 300–309, 2003.
9. Gupta, D., Tator, C.H., and Shoichet, M.S. Fast-gelling injectable blend of hyaluronan and methylcellulose for intrathecal, localized delivery to the injured spinal cord. Biomaterials **27**(11), 2370–2379, 2006.
10. Constantini, S., and Young, W. The effects of methylprednisolone and the ganglioside GM1 on acute spinal cord injury in rats. J Neurosurg **80**(1), 97–111, 1994.
11. Fehlings, M.G. Editorial: recommendations regarding the use of methylprednisolone in acute spinal cord injury: making sense out of the controversy. Spine **26**(24 Suppl), S56–S57, 2001.
12. Hurlbert, R.J. The role of steroids in acute spinal cord injury: an evidence-based analysis. Spine **26**(24 Suppl), S39–S46, 2001.
13. Celik, M., Gokmen, N., Erbayraktar, S., Akhisaroglu, M., Konakc, S., Ulukus, C., Genc, S., Genc, K., Sagiroglu, E., Cerami, A., and Brines, M. Erythropoietin prevents motor neuron apoptosis and neurologic disability in experimental spinal cord ischemic injury. Proc Natl Acad Sci USA **99**(4), 2258–2263, 2002.
14. Ray, S.K., Matzelle, D.D., Sribnick, E.A., Guyton, M.K., Wingrave, J.M., and Banik, N.L. Calpain inhibitor prevented apoptosis and maintained transcription of proteolipid protein and myelin basic protein genes in rat spinal cord injury. J Chem Neuroanat **26**(2), 119–124, 2003.
15. Kigerl, K.A., Lai, W., Rivest, S., Hart, R.P., Satoskar, A.R., and Popovich, P.G. Toll-like receptor (TLR)-2 and TLR-4 regulate inflammation, gliosis, and myelin sparing after spinal cord injury. J Neurochem **102**(1), 37–50, 2007.
16. Tamura, M., Nakamura, M., Ogawa, Y., Toyama, Y., Miura, M., and Okano, H. Targeted expression of anti-apoptotic

protein p35 in oligodendrocytes reduces delayed demyelination and functional impairment after spinal cord injury. Glia **51**(4), 312–321, 2005.

17. Qiao, F., Atkinson, C., Song, H., Pannu, R., Singh, I., and Tomlinson, S. Complement plays an important role in spinal cord injury and represents a therapeutic target for improving recovery following trauma. Am J Pathol **169**(3), 1039–1047, 2006.

18. Pannu, R., and Singh, I. Pharmacological strategies for the regulation of inducible nitric oxide synthase: neurodegenerative versus neuroprotective mechanisms. Neurochem Int **49**(2), 170–182, 2006.

19. Bernaudin, M., Marti, H.H., Roussel, S., Divoux, D., Nouvelot, A., MacKenzie, E.T., and Petit, E. A potential role for erythropoietin in focal permanent cerebral ischemia in mice. J Cereb Blood Flow Metab **19**(6), 643–651, 1999.

20. Siren, A.L., Knerlich, F., Poser, W., Gleiter, C.H., Bruck, W., and Ehrenreich, H. Erythropoietin and erythropoietin receptor in human ischemic/hypoxic brain. Acta Neuropathol **101**(3), 271–276, 2001.

21. Demers, E.J., McPherson, R.J., and Juul, S.E. Erythropoietin protects dopaminergic neurons and improves neurobehavioral outcomes in juvenile rats after neonatal hypoxia-ischemia. Pediatr Res **58**(2), 297–301, 2005.

22. Aydin, A., Genc, K., Akhisaroglu, M., Yorukoglu, K., Gokmen, N., and Gonullu, E. Erythropoietin exerts neuroprotective effect in neonatal rat model of hypoxic-ischemic brain injury. Brain Dev **25**(7), 494–498, 2003.

23. Ehrenreich, H., Hasselblatt, M., Dembowski, C., Cepek, L., Lewczuk, P., Stiefel, M., Rustenbeck, H.H., Breiter, N., Jacob, S., Knerlich, F., Bohn, M., Poser, W., Ruther, E., Kochen, M., Gefeller, O., Gleiter, C., Wessel, T.C., De Ryck, M., Itri, L., Prange, H., Cerami, A., Brines, M., and Siren, A.L. Erythropoietin therapy for acute stroke is both safe and beneficial. Mol Med **8**(8), 495–505, 2002.

24. Grasso, G., Sfacteria, A., Meli, F., Fodale, V., Buemi, M., and Iacopino, D.G. Neuroprotection by erythropoietin administration after experimental traumatic brain injury. Brain Res **1182**, 99–105, 2007.

25. Gorio, A., Gokmen, N., Erbayraktar, S., Yilmaz, O., Madaschi, L., Cichetti, C., Di Giulio, A.M., Vardar, E., Cerami, A., and Brines, M. Recombinant human erythropoietin counteracts secondary injury and markedly enhances neurological recovery from experimental spinal cord trauma. Proc Natl Acad Sci USA **99**(14), 9450–9455, 2002.

26. Kaptanoglu, E., Solaroglu, I., Okutan, O., Surucu, H.S., Akbiyik, F., and Beskonakli, E. Erythropoietin exerts neuroprotection after acute spinal cord injury in rats: effect on lipid peroxidation and early ultrastructural findings. Neurosurg Rev **27**(2), 113–120, 2004.

27. Agnello, D., Bigini, P., Villa, P., Mennini, T., Cerami, A., Brines, M.L., and Ghezzi, P. Erythropoietin exerts an anti-inflammatory effect on the CNS in a model of experimental autoimmune encephalomyelitis. Brain Res **952**(1), 128–134, 2002.

28. Villa, P., Bigini, P., Mennini, T., Agnello, D., Laragione, T., Cagnotto, A., Viviani, B., Marinovich, M., Cerami, A., Coleman, T.R., Brines, M., and Ghezzi, P. Erythropoietin selectively attenuates cytokine production and inflammation in cerebral ischemia by targeting neuronal apoptosis. J Exp Med **198**(6), 971–975, 2003.

29. Diaz, Z., Assaraf, M.I., Miller, W.H., Jr., and Schipper, H.M. Astroglial cytoprotection by erythropoietin pre-conditioning: implications for ischemic and degenerative CNS disorders. J Neurochem **93**(2), 392–402, 2005.

30. Sugawa, M., Sakurai, Y., Ishikawa-Ieda, Y., Suzuki, H., and Asou, H. Effects of erythropoietin on glial cell development; oligodendrocyte maturation and astrocyte proliferation. Neurosci Res **44**(4), 391–403, 2002.

31. Konishi, Y., Chui, D.H., Hirose, H., Kunishita, T., and Tabira, T. Trophic effect of erythropoietin and other hematopoietic factors on central cholinergic neurons *in vitro* and *in vivo*. Brain Res **609**(1–2), 29–35, 1993.

32. Masuda, S., Okano, M., Yamagishi, K., Nagao, M., Ueda, M., and Sasaki, R. A novel site of erythropoietin production. Oxygen-dependent production in cultured rat astrocytes. J Biol Chem **269**(30), 19488–19493, 1994.

33. Brines, M.L., Ghezzi, P., Keenan, S., Agnello, D., de Lanerolle, N.C., Cerami, C., Itri, L.M., and Cerami, A. Erythropoietin crosses the blood–brain barrier to protect against experimental brain injury. Proc Natl Acad Sci USA **97**(19), 10526–10531, 2000.

34. Prestwich, G.D., Marecak, D.M., Marecek, J.F., Vercruysse, K.P., and Ziebell, M.R. Controlled chemical modification of hyaluronic acid: synthesis, applications, and biodegradation of hydrazide derivatives. J Control Release **53**(1–3), 93–103, 1998.

35. Hermanson, G. Bioconjugate Techniques. Second edition, San Diego, CA: Academic Press, 1996.

36. Rivlin, A.S., and Tator, C.H. Effect of duration of acute spinal cord compression in a new acute cord injury model in the rat. Surg Neurol **10**(1), 38–43, 1978.

37. Basso, D.M., Beattie, M.S., and Bresnahan, J.C. A sensitive and reliable locomotor rating scale for open field testing in rats. J Neurotrauma **12**(1), 1–21, 1995.

38. Poon, P.C., Gupta, D., Shoichet, M.S., and Tator, C.H. Clip compression model is useful for thoracic spinal cord injuries: histologic and functional correlates. Spine **32**(25), 2853–2859, 2007.

39. Ritger, P.L., and Peppas, N.A. A simple equation for description of solute release I. Fickian and non-fickian release from non-swellable devices in the form of slabs, spheres, cylinders or discs. J Control Release **5**(1), 23–36, 1987.

40. Narasimhan, B., and Peppas, N.A. Molecular analysis of drug delivery systems controlled by dissolution of the polymer carrier. J Pharm Sci **86**(3), 297–304, 1997.

41. Kwon, B.K., Tetzlaff, W., Grauer, J.N., Beiner, J., and Vaccaro, A.R. Pathophysiology and pharmacologic treatment of acute spinal cord injury. Spine J **4**(4), 451–464, 2004.

42. Carlson, G.D., and Gorden, C. Current developments in spinal cord injury research. Spine J **2**(2), 116–128, 2002.

43. Belazs, E. Medical applications of hyaluronan and its derivatives. In: Gebelein, C., ed. Cosmetic and Pharmaceutical Applications of Polymers. New York: Plenum Press, 293–310, 1991.

44. Mann, C., Lee, J.H., Liu, J., Stammers, A.M., Sohn, H.M., Tetzlaff, W., and Kwon, B.K. Delayed treatment of spinal cord injury with erythropoietin or darbepoetin—a lack of neuroprotective efficacy in a contusion model of cord injury. Exp Neurol **211**(1), 34–40, 2008.

45. Deen, W. Analysis of transport phenomena. In: Gubbins, K.E., ed. Topics in Chemical Engineering. New York: Oxford University Press, 86–91, 1998.

46. Stroh, M., Zipfel, W.R., Williams, R.M., Webb, W.W., and Saltzman, W.M. Diffusion of nerve growth factor in rat

striatum as determined by multiphoton microscopy. Biophys J **85**(1), 581–588, 2003.

47. Loth, F., Yardimci, M.A., and Alperin, N. Hydrodynamic modeling of cerebrospinal fluid motion within the spinal cavity. J Biomech Eng **123**(1), 71–79, 2001.

48. Delpech, B., Bertrand, P., and Chauzy, C. An indirect enzymoimmunological assay for hyaluronidase. J Immunol Methods **104**(1–2), 223–229, 1987.

49. Laurent, U.B., Laurent, T.C., Hellsing, L.K., Persson, L., Hartman, M., and Lilja, K. Hyaluronan in human cerebrospinal fluid. Acta Neurol Scand **94**(3), 194–206, 1996.

50. Stohlman, Jr., F., Ebbe, S., Morse, B., Howard, D., and Donovan, J. Regulation of erythropoiesis. XX. Kinetics of red cell production. Ann NY Acad Sci **149**(1), 156–172, 1968.

51. Morishita, E., Masuda, S., Nagao, M., Yasuda, Y., and Sasaki, R. Erythropoietin receptor is expressed in rat hippocampal and cerebral cortical neurons, and erythropoietin prevents *in vitro* glutamate-induced neuronal death. Neuroscience **76**(1), 105–116, 1997.

52. Yalcin, M., Ak, F., Cangul, I.T., and Erturk, M. The effect of centrally administered erythropoietin on cardiovascular and respiratory system of anaesthetized rats. Auton Neurosci **134**(1–2), 1–7, 2007.

53. Chen, G., Shi, J.X., Hang, C.H., Xie, W., Liu, J., and Liu, X. Inhibitory effect on cerebral inflammatory agents that ac-

company traumatic brain injury in a rat model: a potential neuroprotective mechanism of recombinant human erythropoietin (rhEPO). Neurosci Lett **425**(3), 177–182, 2007.

54. Yatsiv, I., Grigoriadis, N., Simeonidou, C., Stahel, P.F., Schmidt, O.I., Alexandrovitch, A.G., Tsenter, J., and Shohami, E. Erythropoietin is neuroprotective, improves functional recovery, and reduces neuronal apoptosis and inflammation in a rodent model of experimental closed head injury. FASEB J **19**(12), 1701–1703, 2005.

Address reprint requests to:
Molly S. Shoichet, Ph.D.
Centre for Cellular and Biomolecular Research
Room 514, 160 College St.
Toronto
Ontario M5S 3E1
Canada

E-mail: molly.shoichet@utoronto.ca